Supplementary Information (SI) for Journal of Materials Chemistry A.
This journal is © The Royal Society of Chemistry 2026

Bridging Structure and Dynamics: Mechanistic Insights into CMK-3 Incorporated Amide-Hydride Composite System for Solid-State Hydrogen Storage

Supporting information:

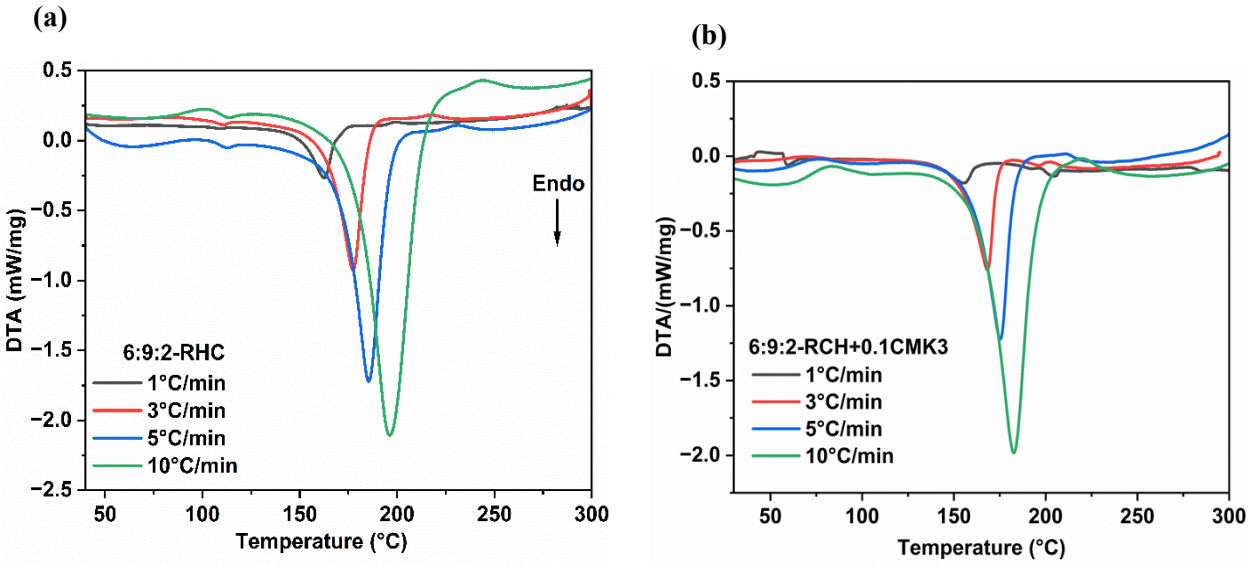

Figure S1. *DTA curves of 6:9:2-RHC at heating rate of 1, 3, 5 and 10 °C/min from RT-300 °C (a), DTA of 6:9:2-RHC+0.1CMK3 at heating rate of 1, 3, 5, 10 °C/min from RT-300 °C (b).*

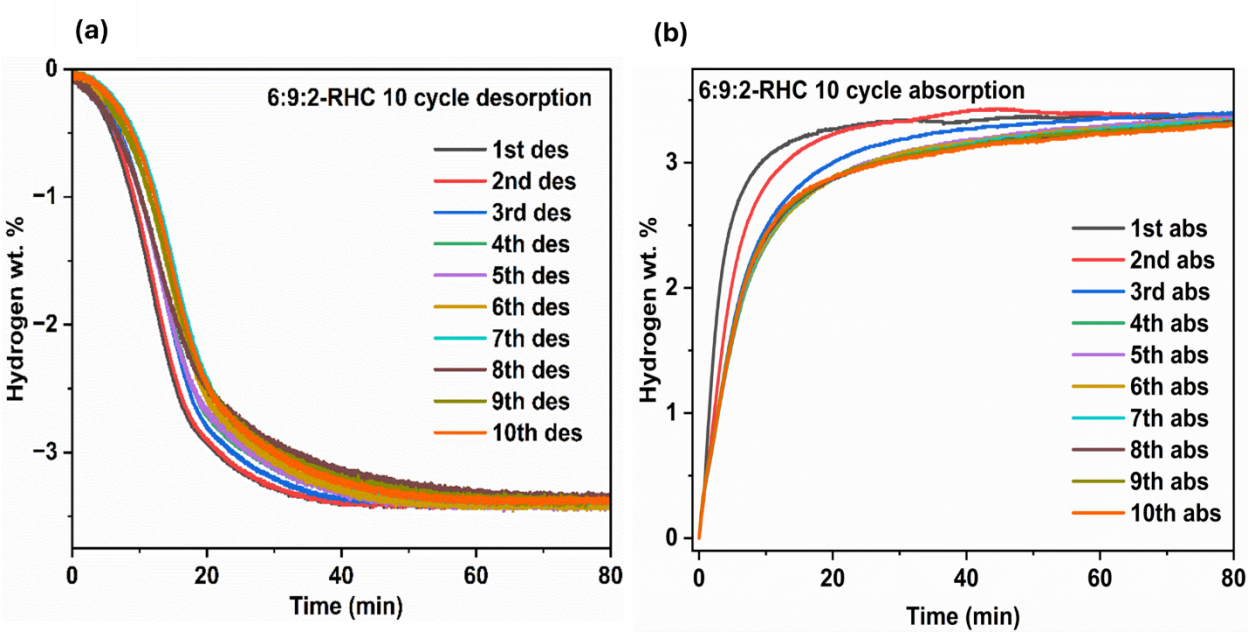

Figure S2*. Isothermal cycling stability of 6:9:2-RHC: 10 hydrogen desorption cycles at 180 °C and 1 bar (a), 10 hydrogen absorption cycles at 180 °C and 80 bar (b).*

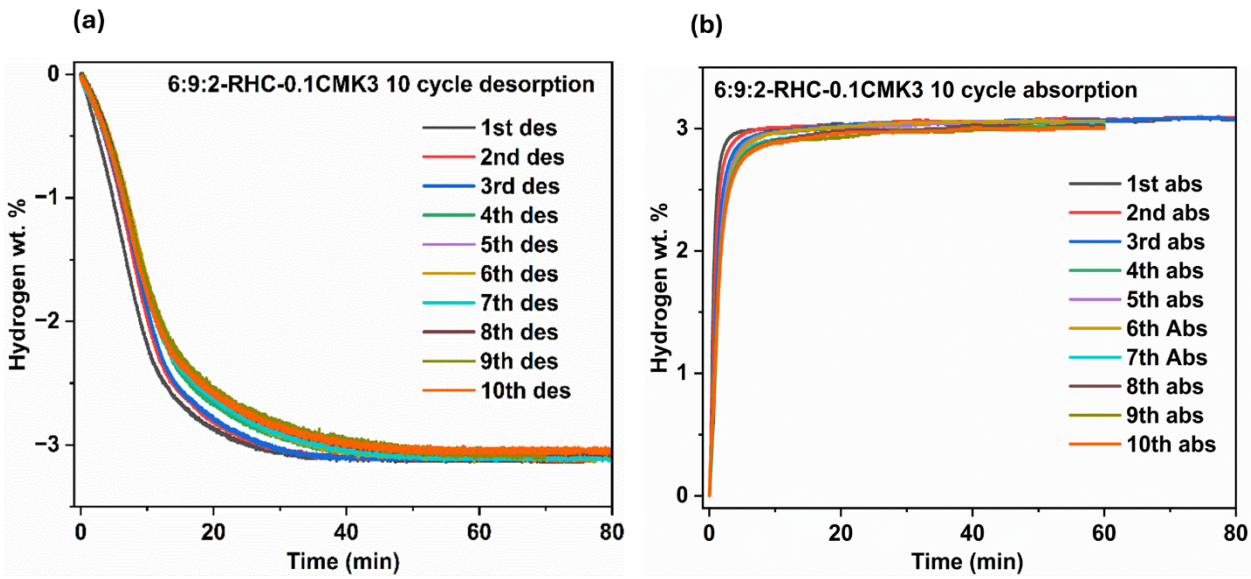

Figure S3. *Isothermal cycling stability of 6:9:2-RHC+0.1CMK3: 10 hydrogen desorption cycles at 180 °C and 1 bar (a), 10 hydrogen absorption cycles at 180 °C and 80 bar (b).*

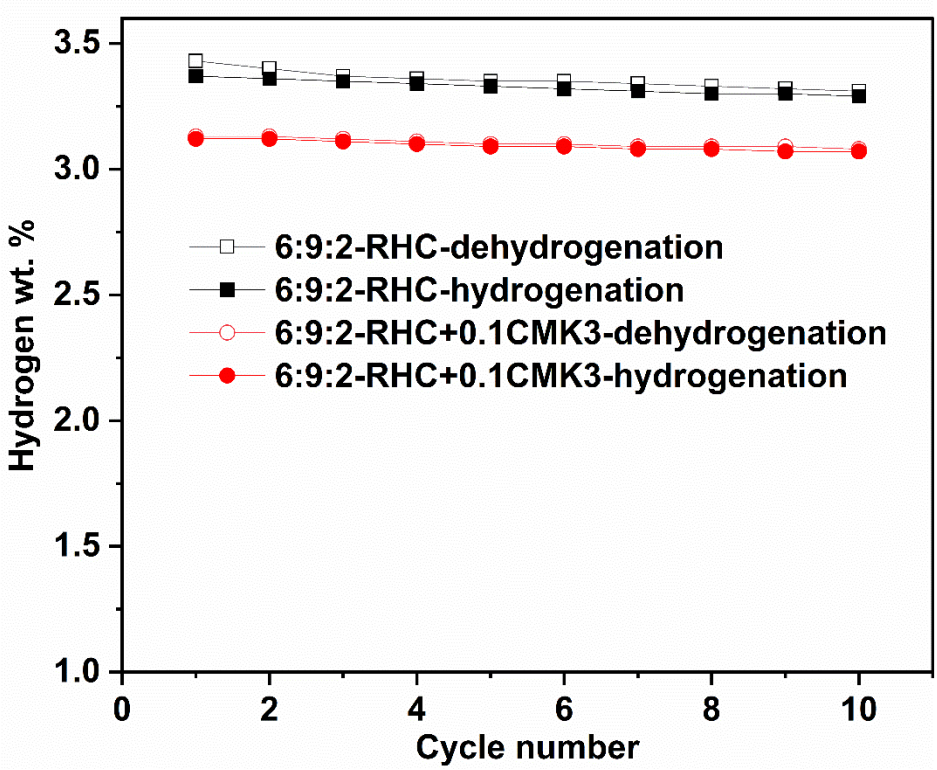

Figure S4. *Hydrogen storage capacity loss of 6:9:2-RHC and 6:9:2-RHC+0.1CMK3 over 10 isothermal cycles of dehydrogenation/hydrogenation.*

Table S1. *Kinetic rate models (JMA) applied in the Sharp-Jones method.*

Kinetic rate models (Diffusion and growth)	Description	Rate equations to be used for Sharp and Jones Method
F1 JMA - n = 1	Interface controlled - 1D growth with interface-controlled reaction rate	$-\ln(1-\alpha)/0.6931$
F2 JMA - n = ½	Diffusion controlled - 2D growth of existent nuclei at constant interface rate	$-\ln(1-\alpha)^{1/2}/0.832$
F3 JMA - n = 1/3	Diffusion controlled - 3D growth of existent nuclei at constant interface rate	$-\ln(1-\alpha)^{1/3}/0.8849$
F4 JMA - n = ¼	Nucleation controlled	$-\ln(1-\alpha)^{1/4}/0.9124$
F5 JMA - n = 2/5	Nucleation and diffusion controlled	$-\ln(1-\alpha)^{2/5}/0.8636$

Fitted kinetic models (F1-F5):

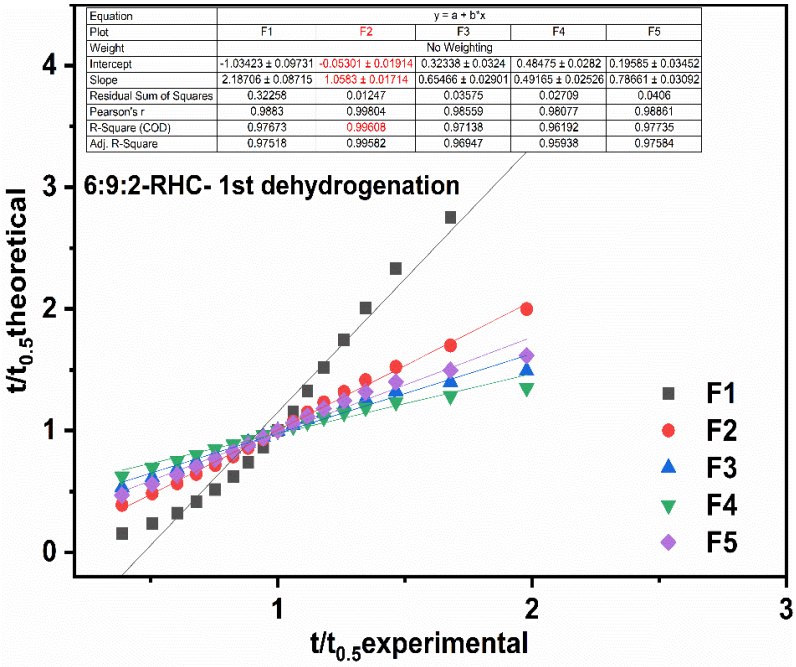

Figure S5. *$t/t_{0.5}$ experimental vs $t/t_{0.5}$ theoretical model fitting using JMA model. 6:9:2-RHC during 1st dehydrogenation follows F2 model.*

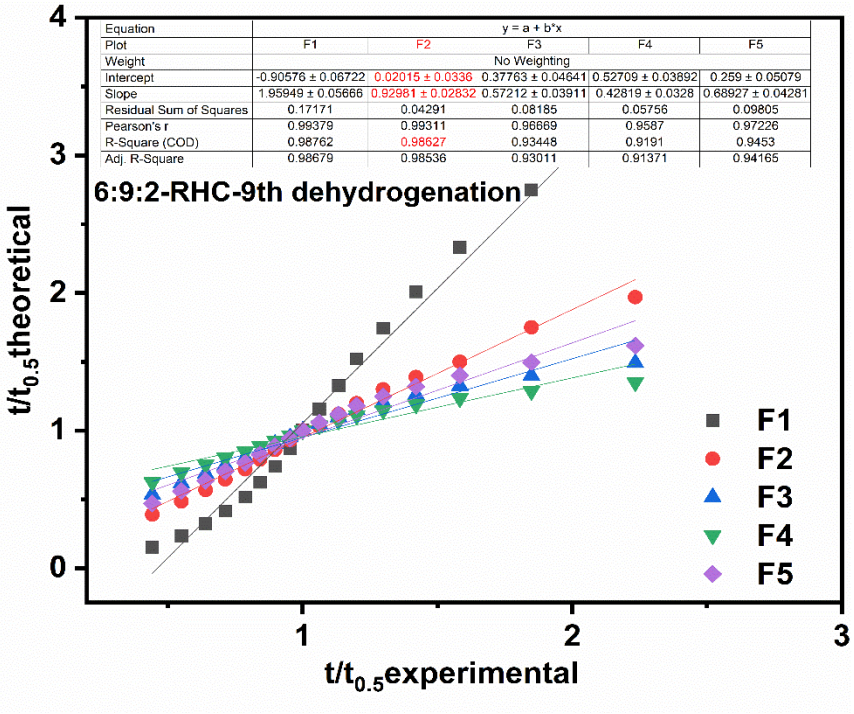

Figure S6. *$t/t_{0.5}$ experimental vs $t/t_{0.5}$ theoretical model fitting using JMA model. 6:9:2-RHC during 9th dehydrogenation follows F2 model.*

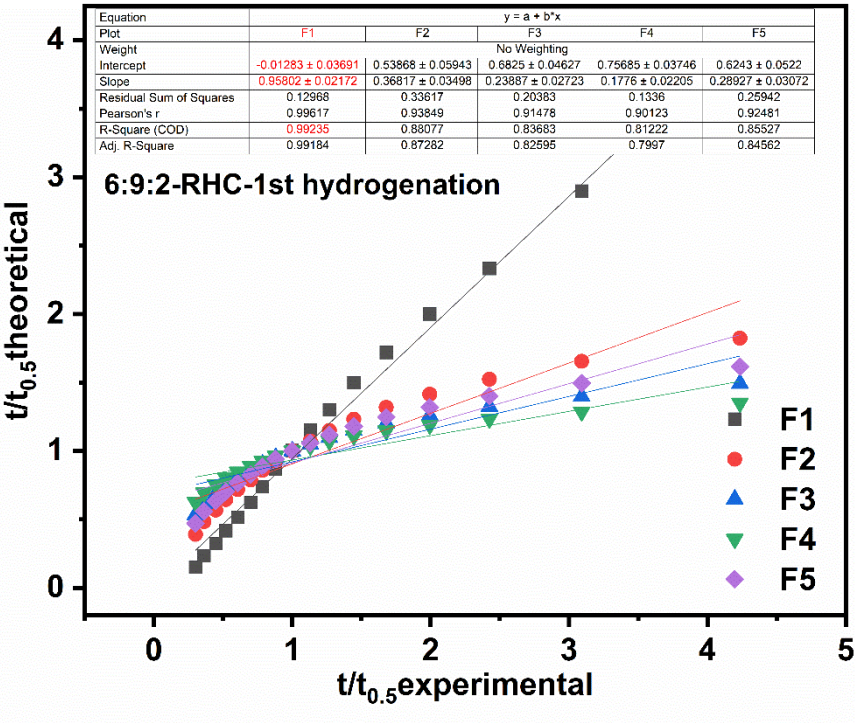

Figure S7. *$t/t_{0.5}$ experimental vs $t/t_{0.5}$ theoretical model fitting using JMA model. 6:9:2-RHC during 1st hydrogenation follows F1 model.*

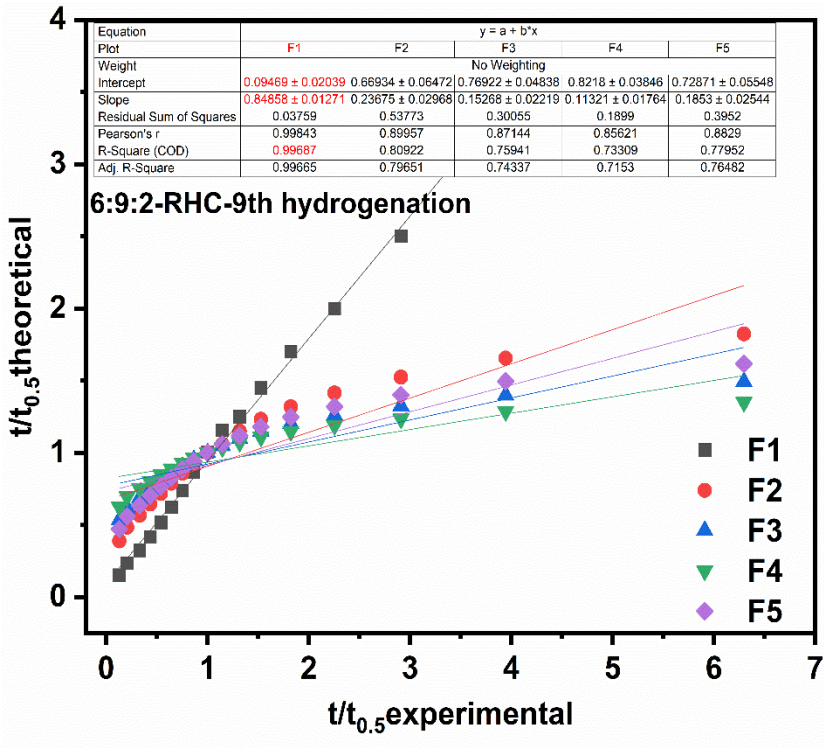

Figure S8. *$t/t_{0.5}$ experimental vs $t/t_{0.5}$ theoretical model fitting using JMA model. 6:9:2-RHC during 9th hydrogenation follows F1 model.*

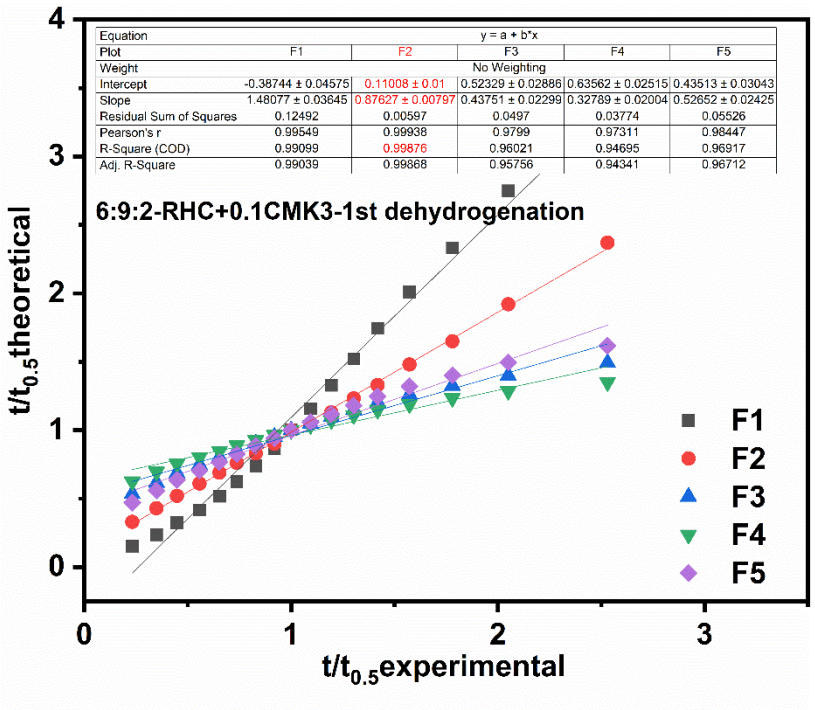

Figure S9. *$t/t_{0.5}$ experimental vs $t/t_{0.5}$ theoretical model fitting using JMA models. 6:9:2-RHC+0.1CMK3 during 1st dehydrogenation follows F2 model.*

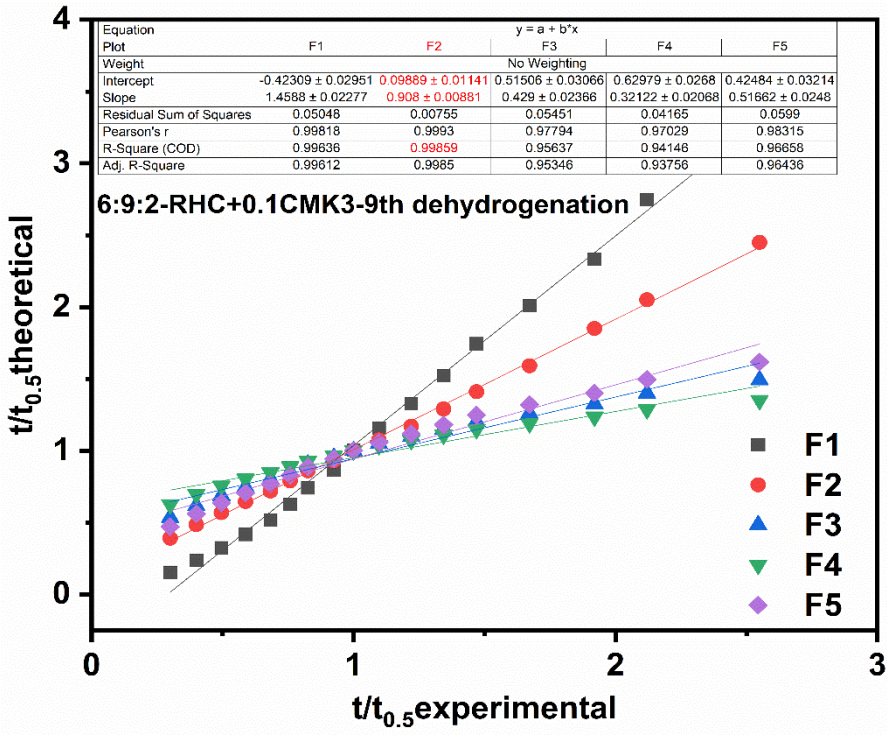

Figure S10. *$t/t_{0.5}$ experimental vs $t/t_{0.5}$ theoretical model fitting using JMA model. 6:9:2-RHC+0.1CMK3 during 9th dehydrogenation follows F2 model.*

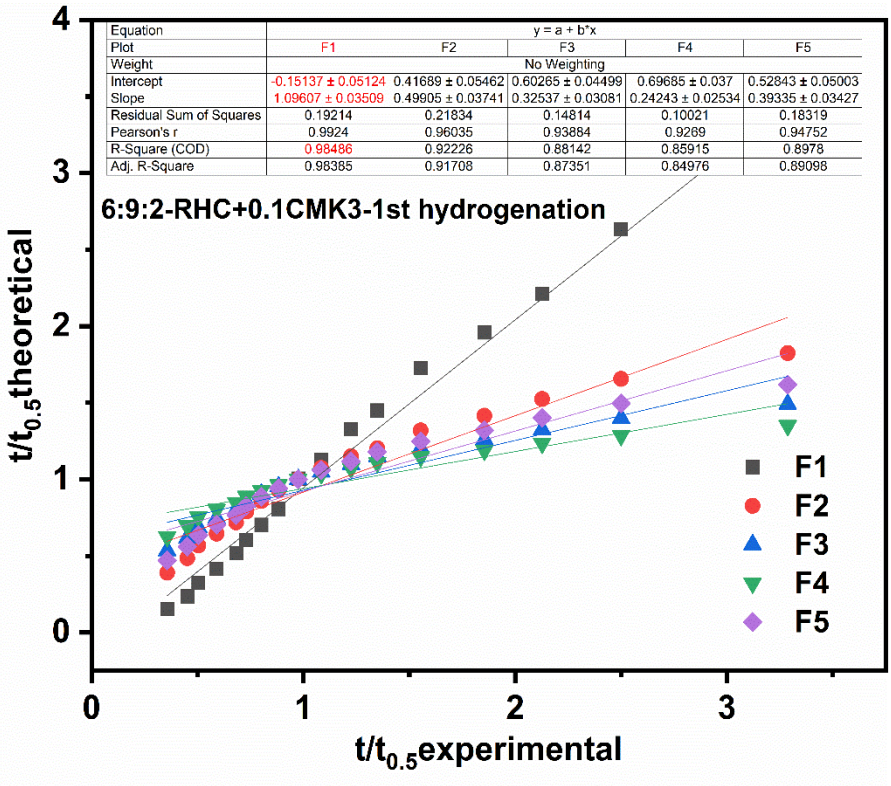

Figure S11. *$t/t_{0.5}$ experimental vs $t/t_{0.5}$ theoretical model fitting using JMA models. 6:9:2-RHC+0.1CMK3 during 1st hydrogenation follows F1 model.*

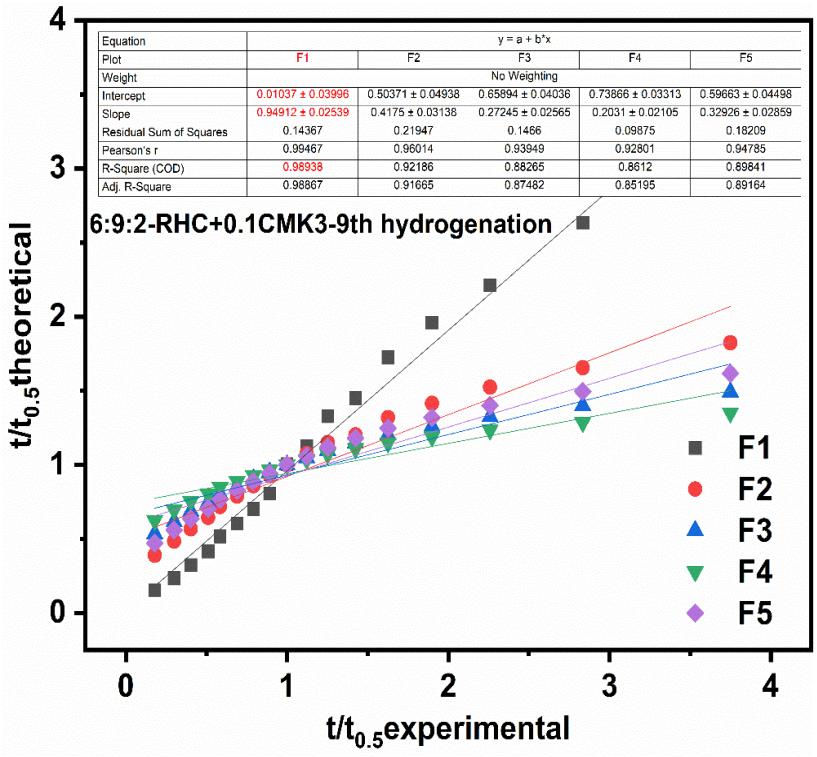

Figure S12. *t/t0.5 experimental vs t/t0.5 theoretical model fitting using JMA model. 6:9:2-RHC+0.1CMK3 9th hydrogenation follow F1 model.*

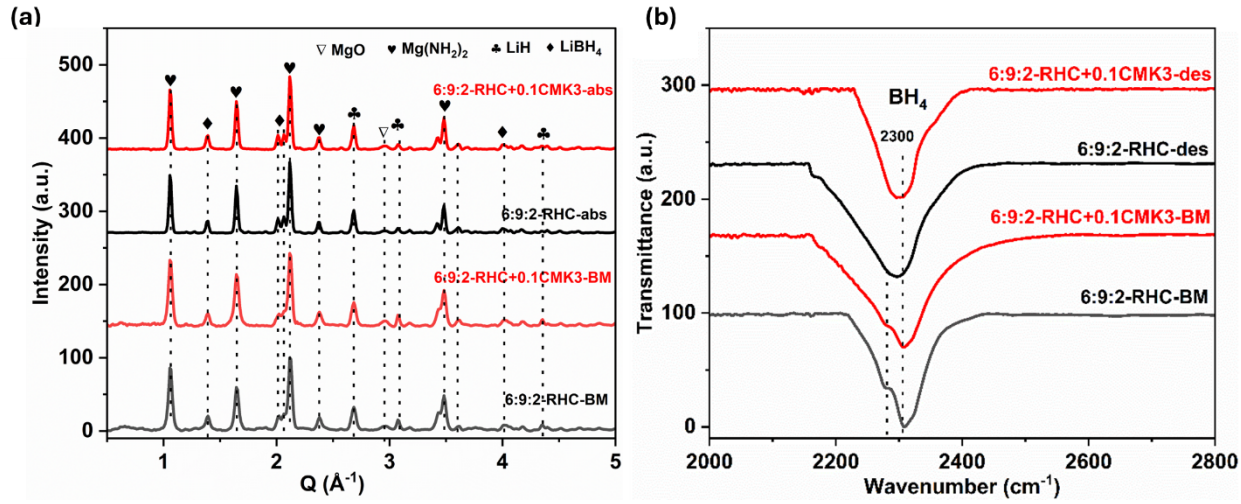

Figure S13. *XRD spectra of 6:9:2-RHC and 6:9:2-RHC+0.1CMK3 both in BM state and after first hydrogen absorption state (a). FTIR spectra of 6:9:2-RHC and 6:9:2-RHC+0.1CMK3 both in BM state and in hydrogen desorption state with focus on BH_4 stretching vibrations (b).*

Table S2. *crystalline size calculation parameters. D= K.λ/β. Cosθ, λ=0.014235 nm, k=0.9*

Sample name / Parameters	***2 θ (degree)***	***FWHM (degree)***	***Crystalline size (nm)***	***Average size (nm)***
6.9.2-BM	*1.37685*	*0.05748*	*12.77136166*	14.07108
	2.13912	*0.05973*	*12.2915251*	
	2.75602	*0.04755*	*15.44179246*	
	3.09035	*0.05505*	*13.33899897*	
	3.99403	*0.04428*	*16.58742043*	
	4.52283	*0.05249*	*13.9953706*	
6.9.2-0.1CMK3-BM	*1.37521*	*0.05717*	*12.8406112*	13.30119188
	1.80565	*0.06482*	*11.32576392*	
	2.13933	*0.05747*	*12.7748881*	
	2.75581	*0.05667*	*12.95671782*	
	3.08946	*0.06634*	*11.06891377*	
	3.48394	*0.06335*	*11.5924904*	
	3.99655	*0.03662*	*20.0571147*	
	4.52302	*0.05326*	*13.79303513*	
6.9.2-desorb	*2.64649*	*0.03735*	*27.61979*	25.38654352
	2.81269	*0.05333*	*19.34436*	
	4.32847	*0.03535*	*29.19548*	
6.9.2-0.1CMK3-desorb	*2.81502*	*0.03858*	*19.03230749*	19.37801288
	4.65394	*0.03977*	*18.4724837*	
	4.48514	*0.03561*	*20.62924744*	

Guinier-Porod model:

$$I(q) = \begin{cases} \frac{G}{Q^s}\exp\left[\frac{-Q^2R_g^2}{3-s}\right] & Q \le Q_1 \\ D/Q^m & Q \ge Q_1 \end{cases}$$

$$Q_1 = \frac{1}{R_g}\sqrt{(m-s)(3-s)/2}$$

$$D = \frac{G}{R_g^{m-s}}\exp\left[-\frac{m-s}{2}\right]\left(\frac{(m-s)(3-s)}{2}\right)^{\frac{m-s}{2}}$$

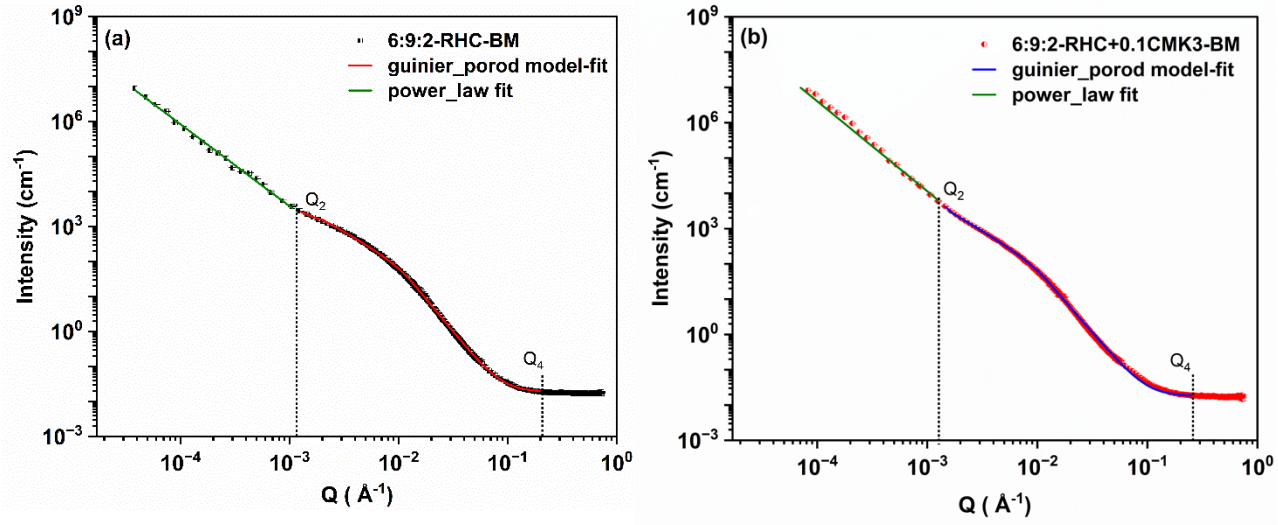

Figure S14. *Power law and Guinier-Porod model fitting on 6:9:2-RHC-BM (a), model fitting on 6:9:2-RHC+0.1CMK3 (b).*

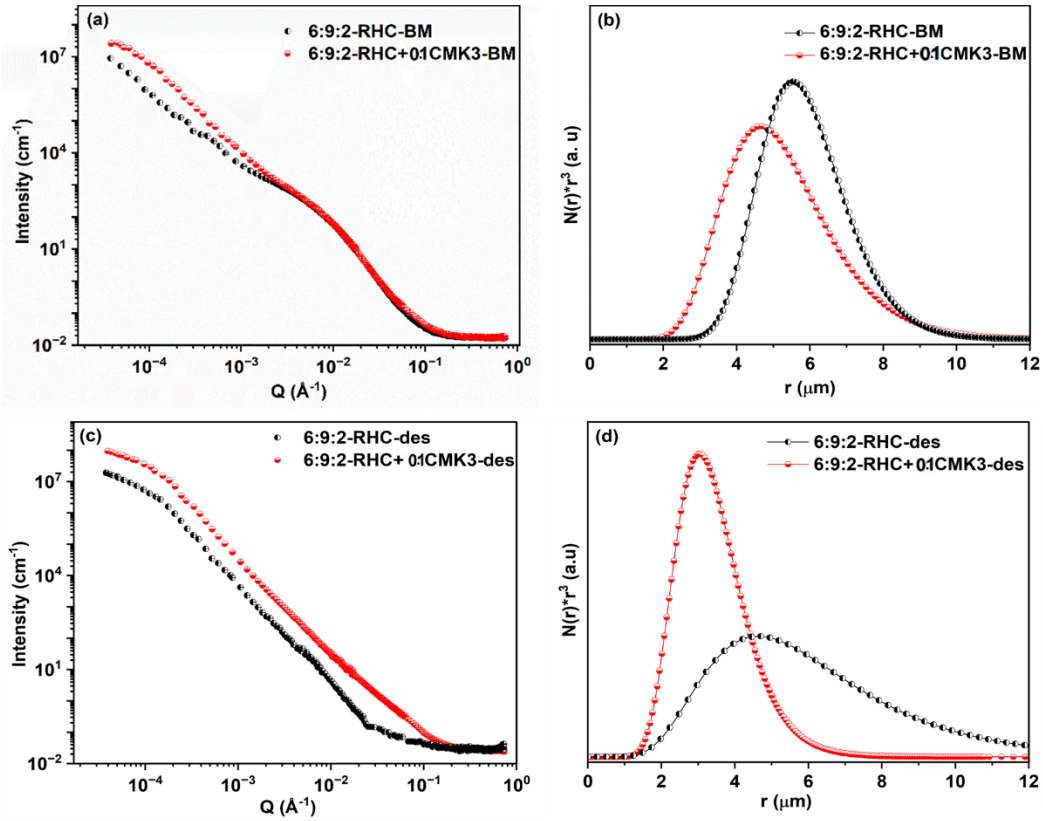

Figure S15. *SANS and USANS data of 6:9:2-RHC and 6:9:2-RHC+0.1CMK3 in ball-milled state and in desorption state (a, c), the particle size calculated after applying Mass Fractal Exp models (b, d).*

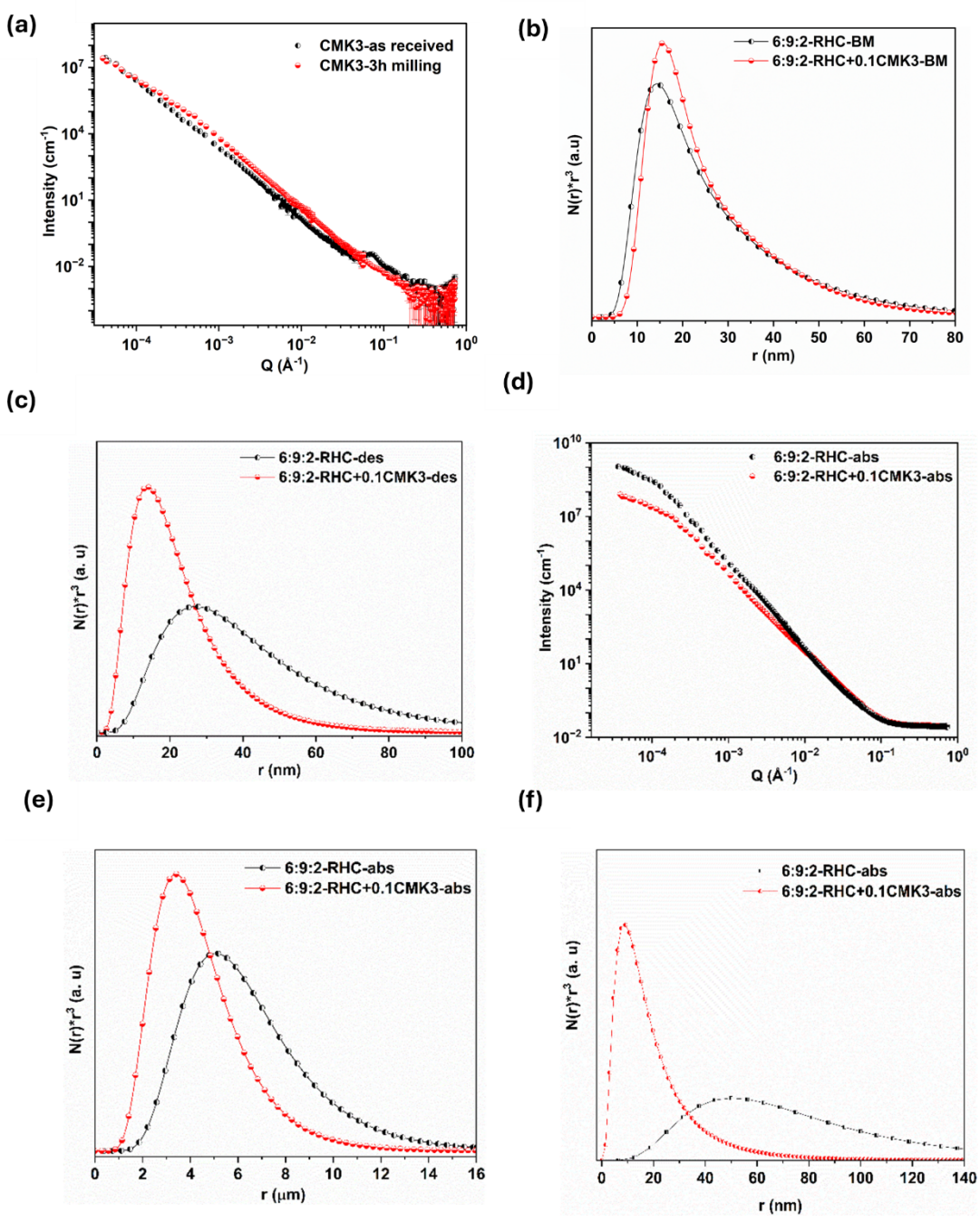

Figure S16. *SANS/USANS data of CMK-3 as received and after milling for reference (a). The grain size calculation of 6:9:2-RHC and 6:9:2-RHC+10CMK3 by using models (b). Similarly, grain size calculation after the desorption state (d). SANS/USANS data of 6:9:2-RHC and 6:9:2-RHC+10CMK3 after first absorption state (c). Particle size calculation and grain size calculation by applying Mass Fractal Exp models (e, f).*

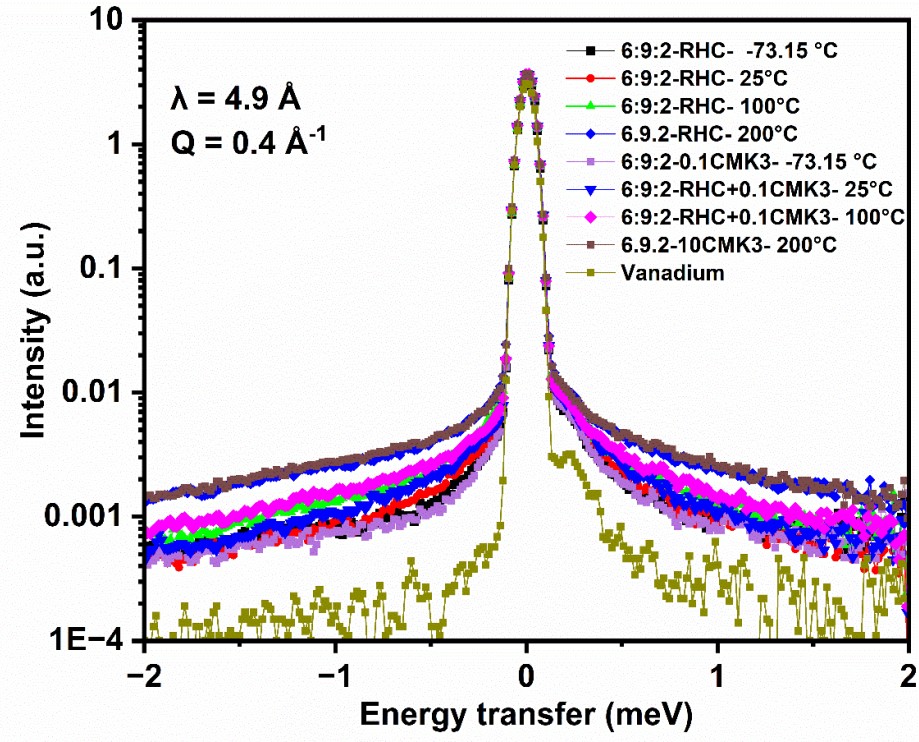

Figure S17. *QENS spectra of 6:9:2-RHC and 6:9:2-0.1CMK3-RHC at different temperatures. Showing a clear broadening around elastic part.*

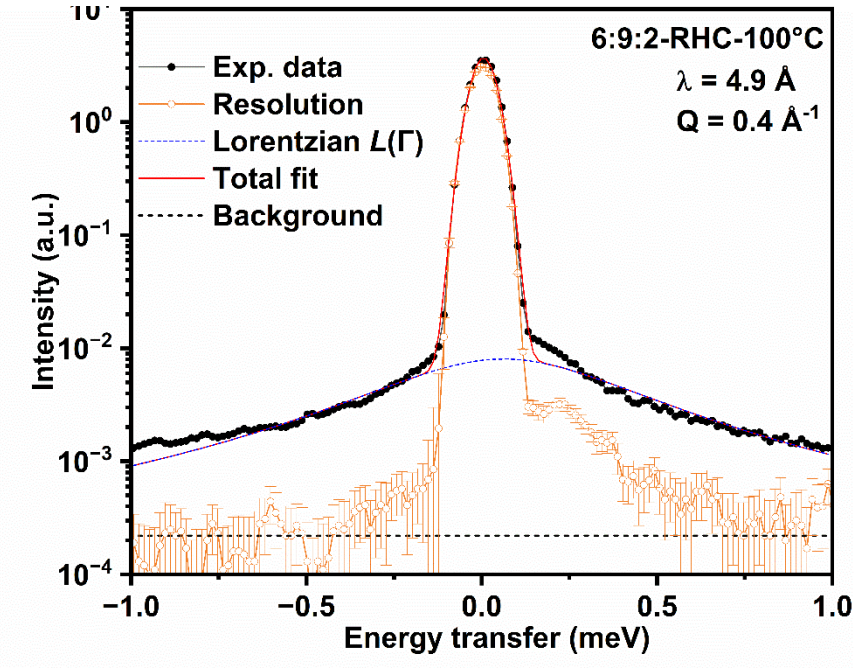

Figure S18. *QENS Model fitted data of 6:9:2-RHC at wavelength of 4.9 Å, using the Lorentzian function, instrumental resolution and background contributions*

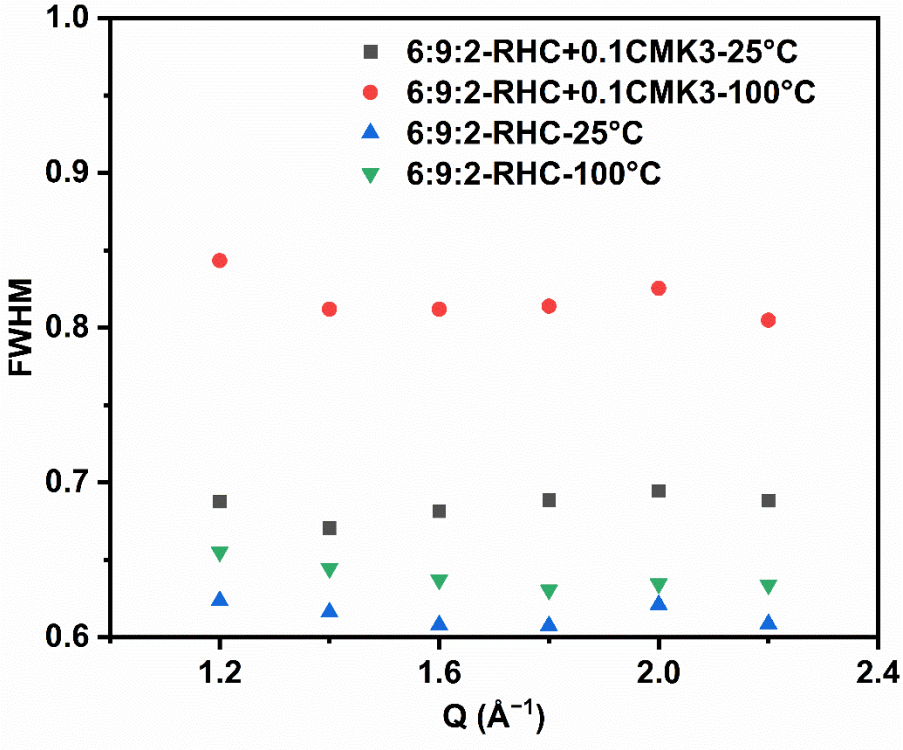

Figure S19. *FWHM vs Q of 6:9:2-RHC and 6:9:2-RHC+0.1CMK3. Showing the Q-dependence of quasielastic broadening*

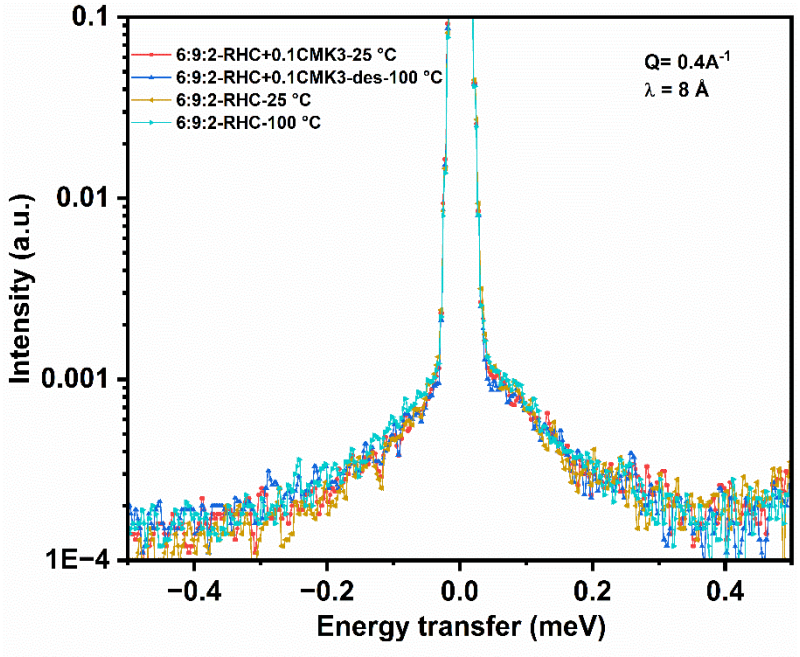

Figure S20. *QENS spectra, energy transfer vs Intensity of 6:9:2-RHC and 6:9:2-RHC+0.1CMK3 at two different temperatures, 8 Å wavelength and at q = 0.4 Å^{-1}.*